

EM Implosion Memos

Memo 38

February 2010

Effect of the impedance of a bicone switch on the focal impulse amplitude and beam width

Prashanth Kumar, Serhat Altunc, Carl E. Baum, Christos G. Christodoulou and Edl Schamiloglu

University of New Mexico

Department of Electrical and Computer Engineering

Albuquerque, NM 87131

Abstract

This paper investigates a vertical bicone antenna as a source and guide for the spherical TEM waves originating from the center. Numerical simulations are used to obtain near-field time-of-arrival measurements for the electric field. Results examining the effect of the switch cone impedance on the focal impulse amplitude and beam width are presented.

1 Introduction

The possibility of using a bicone switch to guide the spherically expanding TEM waves originating from the center, in lieu of the feed arms, was proposed in [1]. This paper investigates such a vertical bicone antenna. The clear times of the electric fields are observed in the near-field to ensure the expanding wavefront is spherical. The effect of the switch cone impedance on the focal impulse amplitude and beam width (spot size) is examined. The impedance of the bicones is varied, from 100Ω to 400Ω , to cover a practically reasonable range.

2 Setup

2.1 Structure visualization

The switch cones and reflector setup, for a 200Ω bicone, is shown in Fig. 2.1. The geometric center of the switch cones is the first focal point. The height of each cone is $h = 6.0$ cm, i.e., $h > ct_\delta = 3.0$ cm.

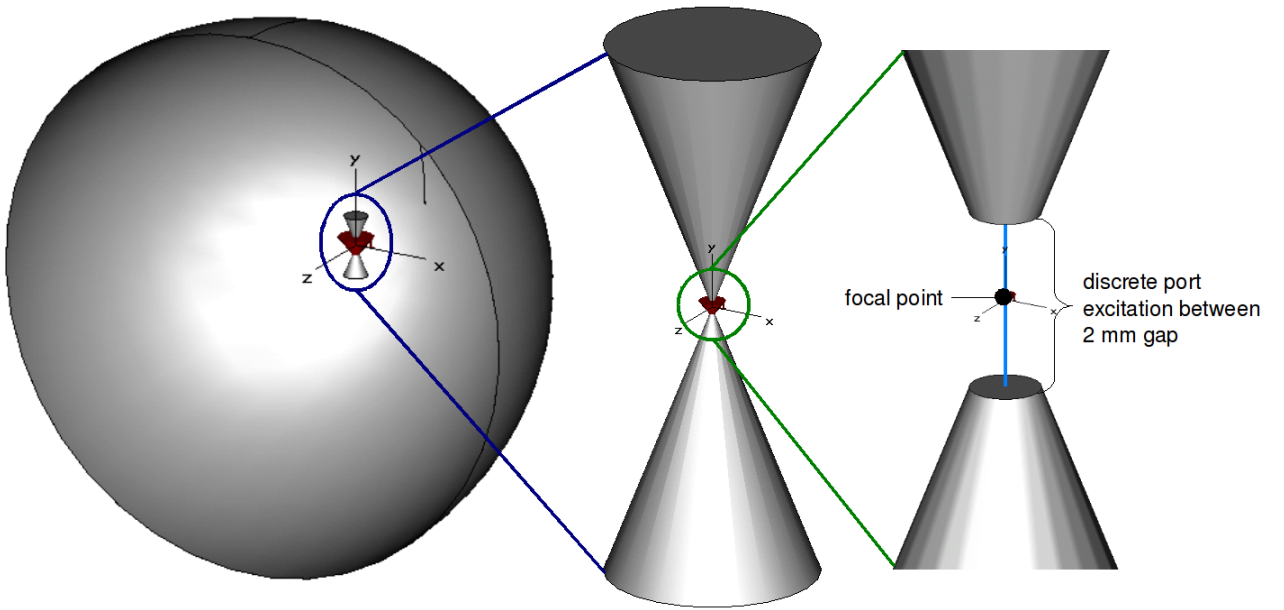


Figure 2.1: Switch bicone and reflector setup. A 1 V excitation is applied between a 2 mm gap in the cones.

In this paper, the bicone impedance is varied to examine its effects on the focal impulse response and the beam width. The impedances are calculated using the relations in [1]. The setup in Fig. 2.1 was used as a template for simulating cones of any impedance, i.e.,

- The geometric center of the switch cones is the first focal point.
- The switch (excitation) gap is 2 mm.

- The height of each cone is $h = 6.0$ cm.

A discrete port, 1 V, 100 ps ramp rising step excitation was applied between the 2 mm gap as shown in Fig. 2.1.

2.2 Electric field probe placements and orientations

A perspective view of the electric field probe placements and orientations is shown in Fig. 2.2. Two sets of electric field probes were used. One set was placed on a (virtual) sphere of radius 10.0 cm centered at the first focal point. These probes were used to monitor the outward propagating wave originating from the switch center. The orientations of these probes are identical to those in [1].

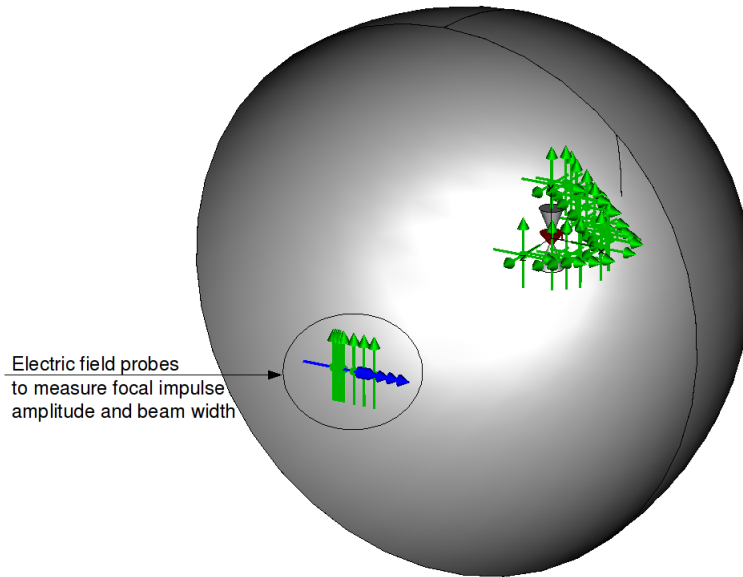


Figure 2.2: Perspective view of the probe placements and orientations at the first and second focal points.

A second set of electric field probes were placed along the x -axis, where $x = 0$ cm corresponds to the second focal point. Probes were placed at $x = 0, 0.25, 0.5, 1.0, 1.25, 1.5, 2.0, 4.0$ and 6.0 cm oriented along $+y$. Magnetic field probes were placed at the same locations and were oriented along $+x$. These probes were used to measure the focal impulse response and beam width.

2.3 Important CST/Simulation Parameters

Domain	Time
Excitation	Discrete
Input	Ramp rising step with 100 ps rise time
Excitation voltage	1 V
Frequency range	0–10 GHz
LPW	10

3 Results

3.1 Time of arrival measurements

One of the advantages of using a vertical bicone antenna is the uniformity of the waves originating from the switch center. This is evidenced by the time-of-arrival measurements, for a $200\ \Omega$ bicone, in Fig. 3.1. Compared to the results in [1], one notes the following differences,

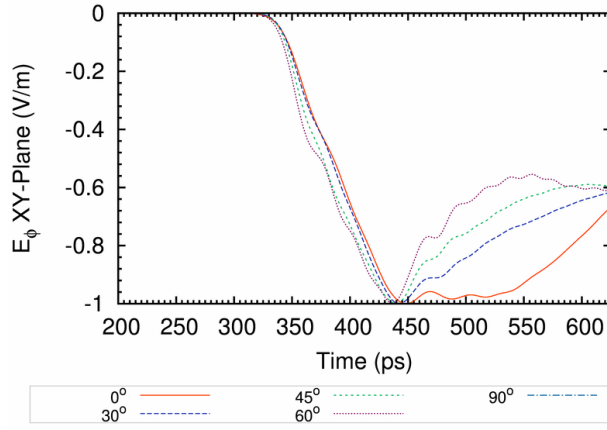
1. The E_θ component in the xy -plane is (nearly) zero. Note that the electric fields in Fig. 3.1(b) are *not* normalized.
2. The time spread in the normalized E_ϕ component in the XY-plane and the normalized E_θ component in the YZ-plane is greater, approximately 10 ps.
3. The peak amplitude of the pre-pulse, for e.g., the E_ϕ component in the XY-plane, is ≈ -4 V/m compared to -12 V/m in [1].

The second difference is most likely due to different simulation parameters. A 25 ps excitation and a frequency range of 0-40 GHz were used in the simulations in [1], while the simulations in this paper use a 100 ps excitation and a frequency range of 0-10 GHz, i.e., the numerical, spatio-temporal, resolution for the simulations in this paper is much lower than the simulations in [1]. The third difference is due to the larger distance of the near-field probes, 10.0 cm, compared to 3.0 cm in [1].

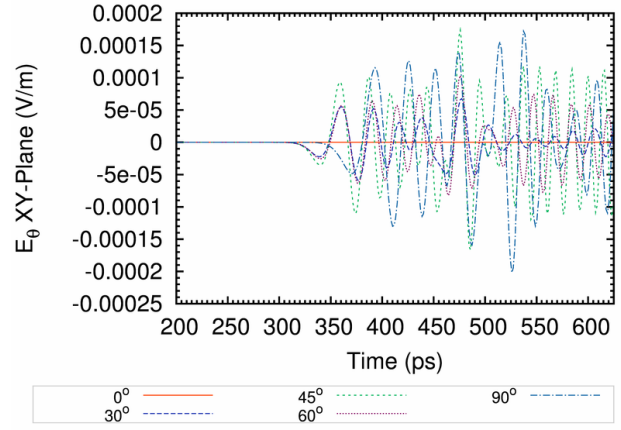
3.2 Variation of switch cone impedance

The focal impulse amplitude and beam width at the second focal point are parameters used to measure the effectiveness of the PSIRA. Figure 3.2 shows the impulse response, at the second focal point, in air, from a $200\ \Omega$ bicone antenna. The most noteworthy feature is the smaller, shorter prepulse due to the geometry of the switch cones. This is very desirable. Note that the circular cone bases “shadow” some area on the top and bottom of the reflector. This reduces the amplitude of the focal impulse. The shape and features of the waveform in Fig. 3.2 are the same for a bicone switch of any impedance.

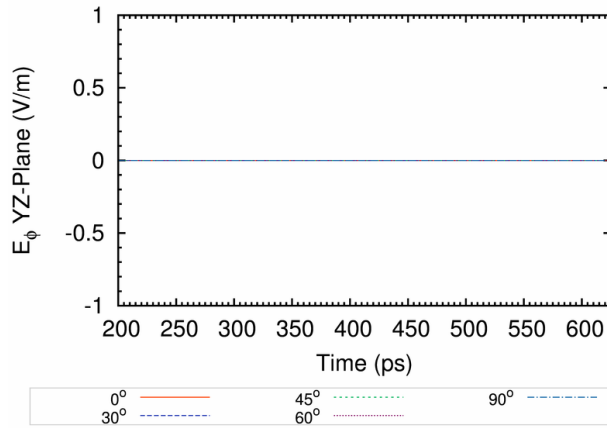
Results for the peak focal impulse amplitude and beam width for various cone impedances are summarized in Table 1 and plotted in Fig. 3.3. As a reference, $E_{\max} = 6.247$ V/m and spot size = 3.610 cm for four feed arms [2]. Detailed plots of the focal waveforms and the spot sizes for each cone impedance are given in the appendix. As seen in Fig. 3.3, the peak impulse amplitude decreases with increase in the bicone impedance, while the spot size increases with increase in the impedance.



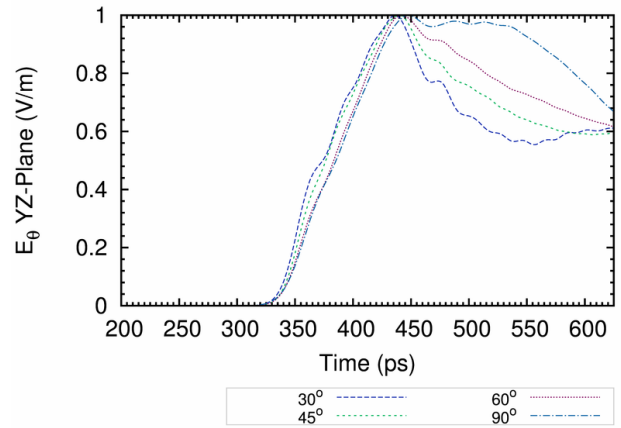
(a) Normalized E_ϕ in the xy -plane



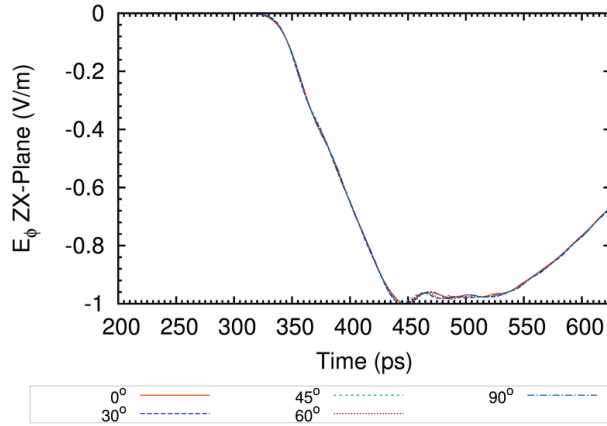
(b) E_θ in the xy -plane



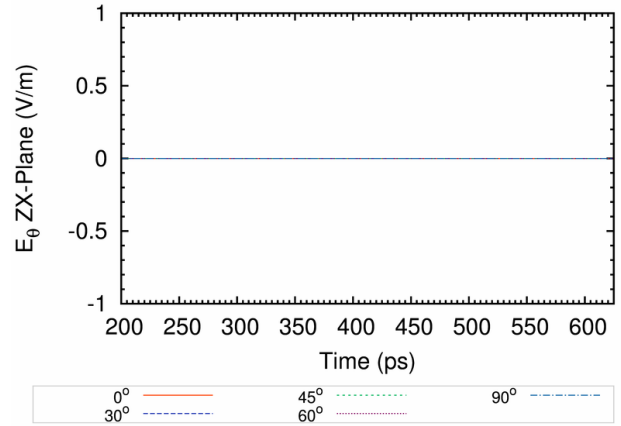
(c) Normalized E_ϕ in the $-yz$ -plane



(d) Normalized E_θ in the $-yz$ -plane



(e) Normalized E_ϕ in the $-zx$ -plane



(f) Normalized E_θ in the $-zx$ plane

Figure 3.1: Normalized E_θ and E_ϕ components of the electric fields from the probes on the xy , $-yz$ and $-zx$ planes for a 200Ω bicone antenna.

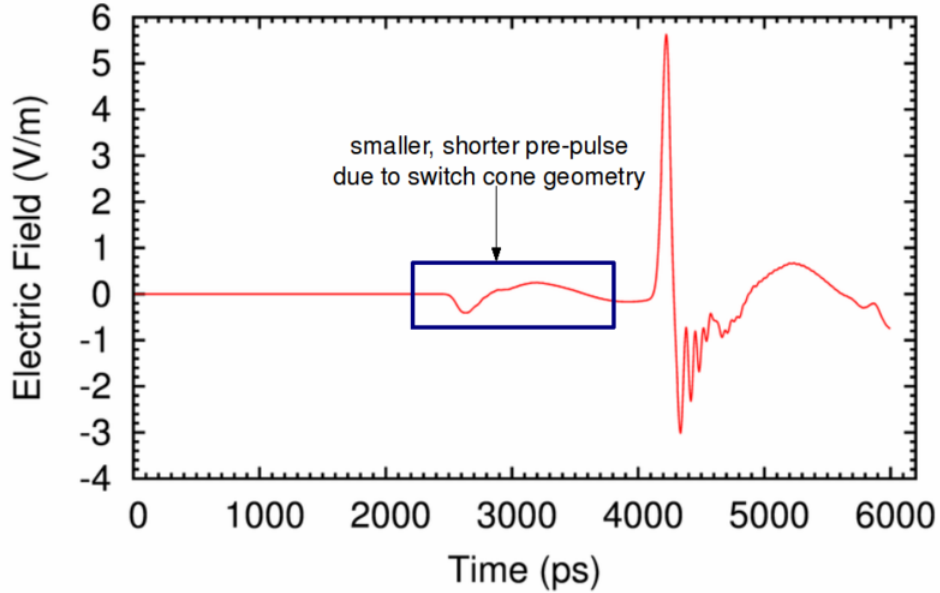


Figure 3.2: Focal impulse waveform for a 200 Ω bicone switch.

Table 1: Peak focal impulse amplitude and beam width for various switch cone impedances.

Z_c (Ohms)*	θ (Deg)	E_{\max} (V/m)	Spot size (cm)
50	46.98	8.117	3.737
75	31.98	6.727	3.894
100	21.37	5.619	4.065
125	14.20	4.708	4.304
150	9.39	4.057	4.414
200	4.09	3.144	4.455

*Bicone impedance = 2 Z_c

3.2.1 Normalization with respect to input power

The input power, P_{in} , for an input voltage, V_{in} , is

$$P_{\text{in}} = \frac{V_{\text{in}}^2}{Z_c}. \quad (3.1)$$

Since $V_{\text{in}} = 1$ V is fixed in all the simulations, the input power is obviously not the same for all the bicones in Table 1 and Fig. 3.3. It is more useful to compare the peak focal impulse amplitudes normalized with respect to the input power. For a fixed input power, the relation between the input voltages for two different cones, say, a and b , is

$$V_{\text{in}}^a = V_{\text{in}}^b \sqrt{\frac{Z_c^a}{Z_c^b}} \Rightarrow E_{\text{max}}^a = E_{\text{max}}^b V_{\text{in}}^a, \quad (3.2)$$

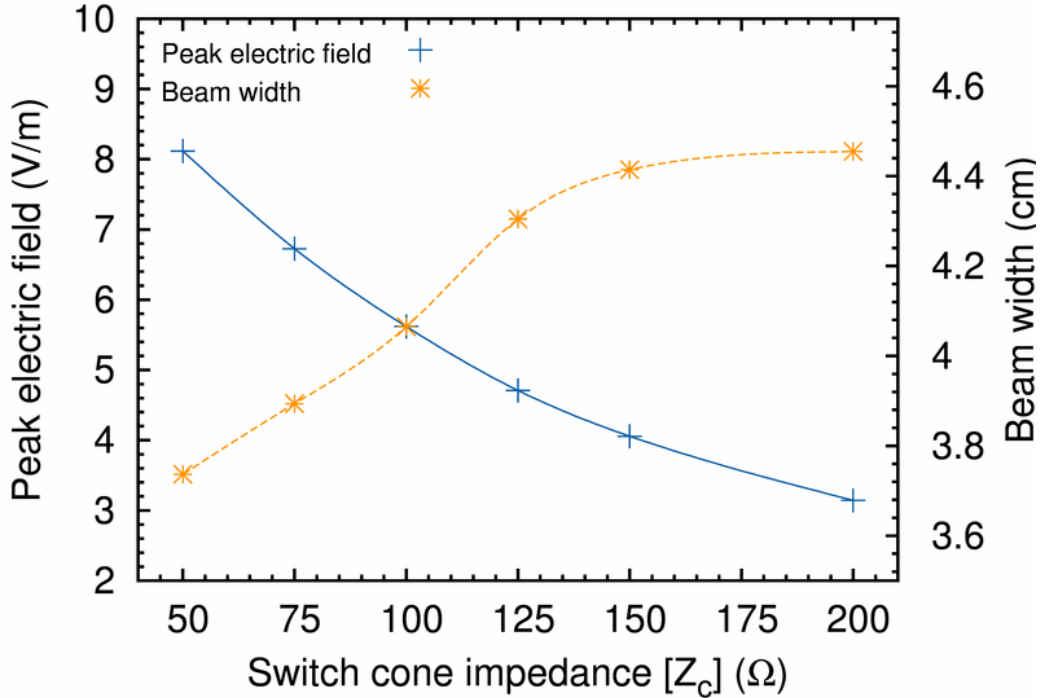


Figure 3.3: Peak focal impulse amplitude and beam width for various switch cone impedances.

where E_{\max}^a is the peak focal impulse amplitude with cone a as the antenna and \mathbb{E}_{\max}^a is the rescaled peak focal impulse amplitude with input voltage V_{in}^a . Let $V_{\text{in}}^b = 1$ V and $Z_c^b = 200$ Ω, i.e., normalize all results with respect to the input power for a 200 Ω cone. Then,

$$V_{\text{in}}^a = \sqrt{\frac{Z_c^a}{200}} \Rightarrow \mathbb{E}_{\max}^a = E_{\max}^a \sqrt{\frac{Z_c^a}{200}}. \quad (3.3)$$

The peak electric field normalized with respect to the input power, **Normalized** E_{\max} , is shown in Fig. 3.4. For a fixed input power, a 75 Ω cone (150 Ω bicone) has the largest peak impulse electric field.

4 Conclusions

Clear time measurements in the near-field indicate that the wavefront expanding from the switch center is approximately spherical with a 10 ps time spread. A finer resolution in our software would likely yield a smaller time spread, but 10 ps is well within the tolerance.

The peak impulse response decreases with increase in the switch cone impedance, while the spot size increases with increase in the switch cone impedance, Fig. 3.3. It would appear that a lower cone impedance is more advantageous as evidenced by the results in Fig. 3.3 and Fig. 3.4. However, the design of the switch system is ultimately dictated by rise time, capacitance, and inductance considerations which are related to the bicone impedance. Optimization of these parameters will play an important role in deciding Z_c . Nevertheless, Fig. 3.3 and Fig. 3.4 serve as a good reference.

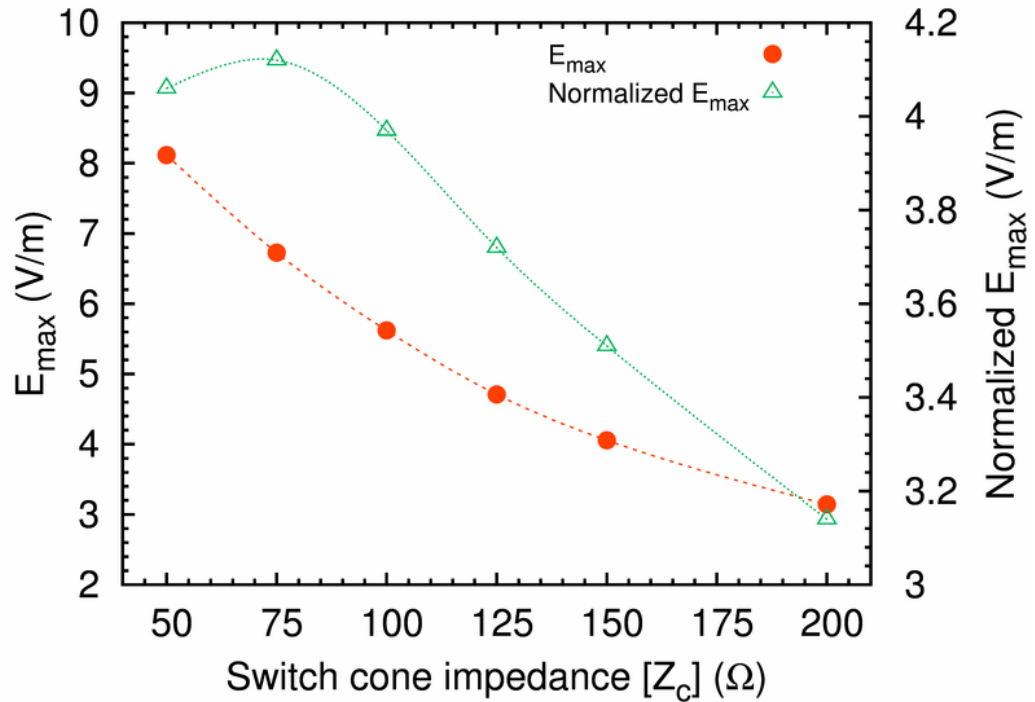


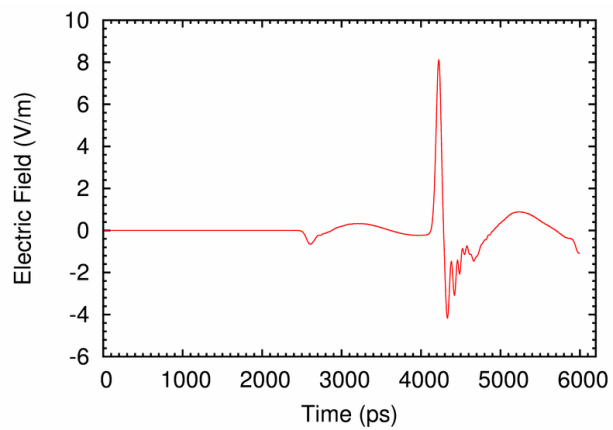
Figure 3.4: E_{\max} and normalized E_{\max} for various switch cone impedances.

References

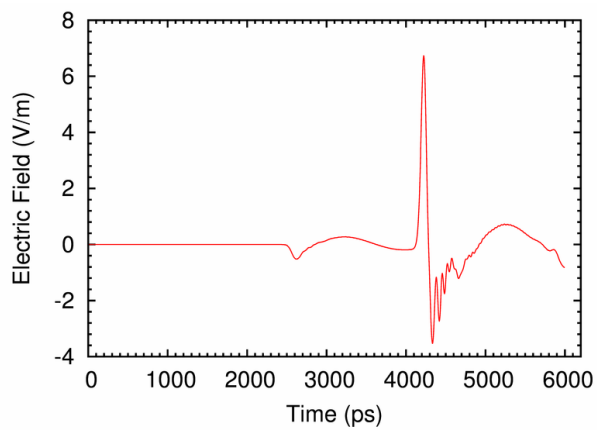
- [1] Prashanth Kumar, Carl E. Baum, Serhat Altunc, Christos G. Christodoulou and Edl Schamiloglu . Near-field time-of-arrival measurements for four feed-arms with a bicone switch. EM Implosion Memo 37, February 2010.
- [2] Prashanth Kumar, Carl E. Baum, Serhat Altunc, Christos G. Christodoulou and Edl Schamiloglu . Numerical simulations of a 60 degree four-feed-arm PSIRA to determine the beam width inside a focusing lens. EM Implosion Memo 35, October 2009.

APPENDIX

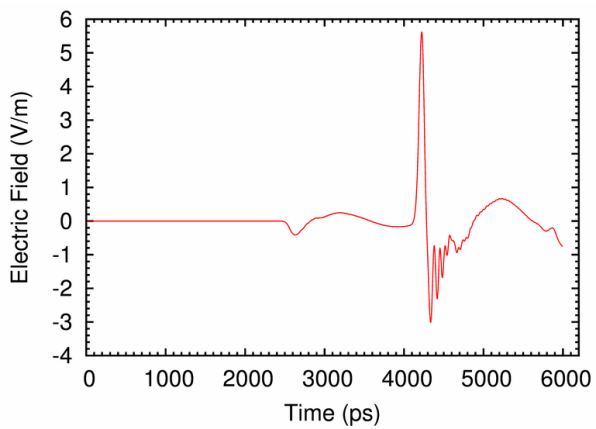
Focal waveform and beam width for various switch cone impedances



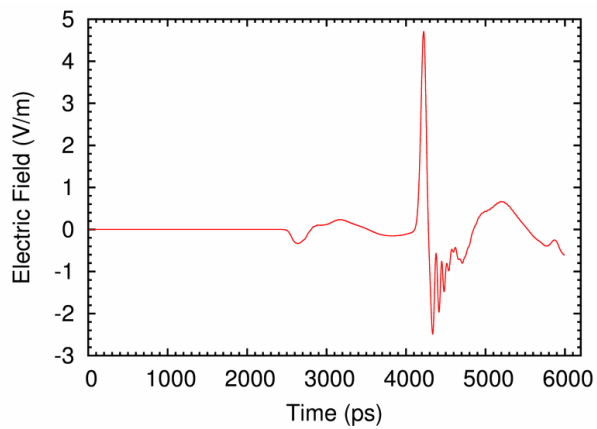
(a) 50Ω



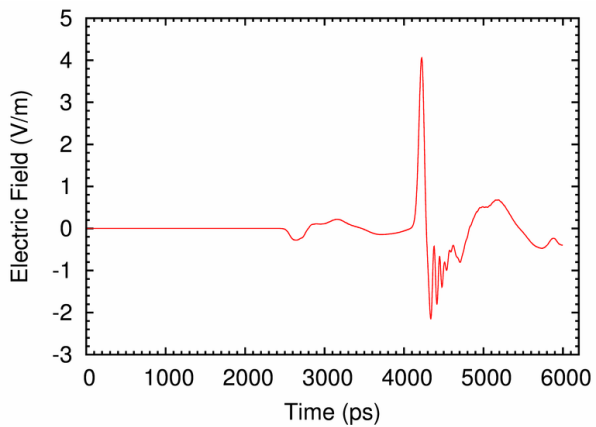
(b) 75Ω



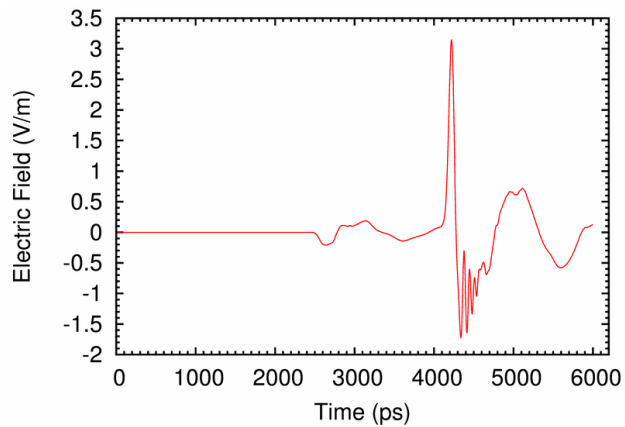
(c) 100Ω



(d) 125Ω

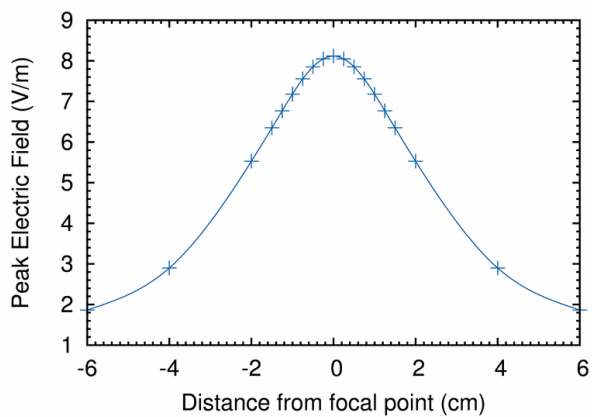


(e) 150Ω

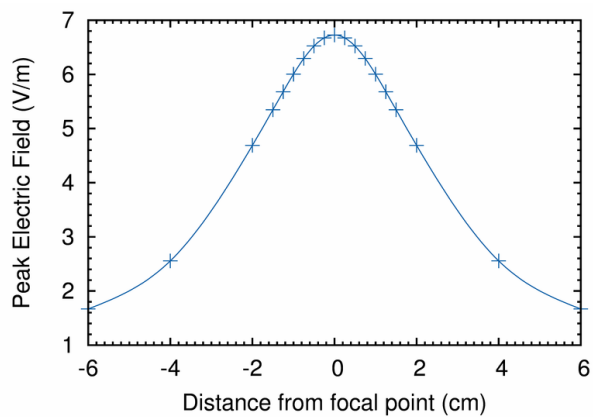


(f) 200Ω

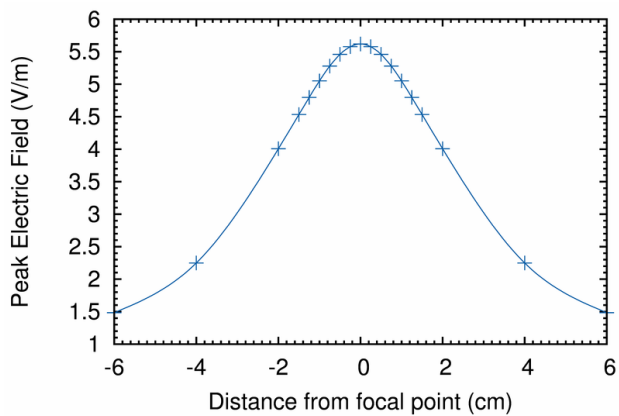
Figure 4.1: Focal impulse waveforms for various cone impedances.



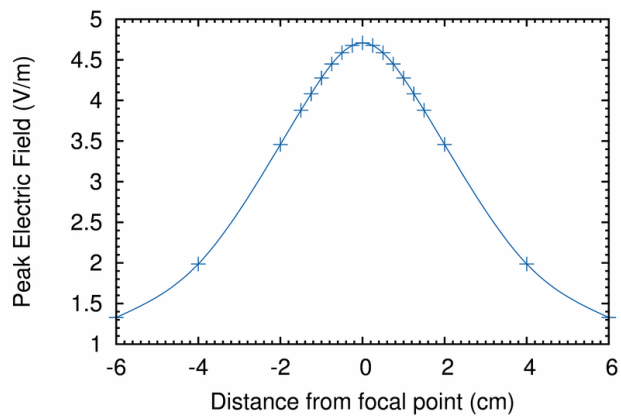
(a) 50 Ω



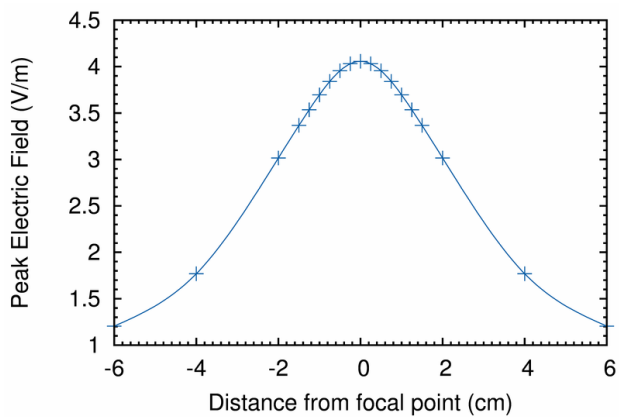
(b) 75 Ω



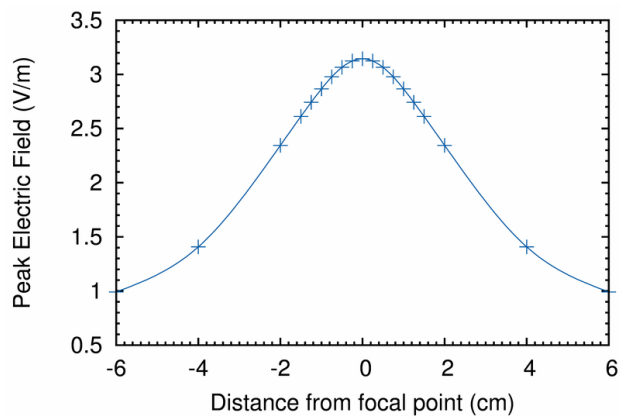
(c) 100 Ω



(d) 125 Ω



(e) 150 Ω



(f) 200 Ω

Figure 4.2: Spot sizes for various cone impedances.